Since January 2020 Elsevier has created a COVID-19 resource centre with free information in English and Mandarin on the novel coronavirus COVID-19. The COVID-19 resource centre is hosted on Elsevier Connect, the company's public news and information website.

Journal of the Indian Chemical Society 99 (2022) 100571

Contents lists available at ScienceDirect

Journal of the Indian Chemical Society

journal homepage: www.journals.elsevier.com/journal-of-the-indian-chemical-society

Molecular docking and dynamic simulation of approved drugs targeting against spike protein (6VXX) of 2019-nCoV (novel coronavirus)

Abhinay Thakur [a], Dikshita Bansode [a], Pragati Ghare [a], Shrutika Sakpal [a,b,*]

[a] Department of Biotechnology, Dr. Homi Bhabha State University, The Institute of Science, 15, Madam Cama Road, Mumbai, 32, Maharashtra, India
[b] Amity Institute of Biotechnology, Amity University Rajasthan, Jaipur, 303002, Rajasthan, India

ARTICLE INFO

Keywords:
SARS-CoV-2 spike protein
Paritaprevir
Molecular docking and dynamic simulation

ABSTRACT

The 2019-nCoV has triggered a global public health emergency due to its rapid spread, resulting in a pandemic situation. Because of its ability to bind with the host cell receptor ACE-2, the spike protein of the 2019-nCoV is a critical factor in viral infection. The current study aims to investigate the molecular-docking of the spike protein (6VXX) using PyRx for FDA-approved drugs available for the treatment of SARS-1 and MERS, with the hypothesis that these drugs could be suggested for the treatment of 2019-nCoV or not. A phylogenetic analysis of 2019-nCoV in relation to SARS-1 and MERS confirmed the validation. The positive result urged the Multiple Sequence Alignment analysis of the top five affected countries, with China serving as a control, using WHO available reference data to determine the rate of mutant variation. The docking results revealed that the top ten drugs with the highest binding affinity rate are also used for Hepatitis-C virus treatment, and the Molecular Dynamic Simulation was carried out for the drug Paritaprevir, which had the highest binding affinity rate, using Gromacs. The results indicated that the drug Paritaprevir could be used as a potential target against the 2019-nCoV Spike protein.

1. Introduction

The 2019-nCoV (novel coronavirus) has emerged globally which is highly transmittable and thus it has been declared as an immediate emergency output as a pandemic by the World Health Organisation (WHO). Coronaviruses cause infections in both humans as well as animals since they are an etiological agent that mostly targets the respiratory tracts leading to difficulty in breathing and systematically too in the digestive tract. Previous studies have reported that Coronavirus has infected several species of animals including mammals, avians, and reptiles. This infective agent was found to have emerged from the town of the city in China's Hubei inflicting fever, severe respiratory problems (difficulty in breathing), lack of odorless, pneumonia-like symptoms, etc. which later termed as COVID-19 by the International Committee on Taxonomy of Viruses (ICTV) thereby leading lakhs of death globally [1–3] (see Table 1).

1.1. Classification of Virus based on ICTV [4]

➢ **Super Kingdom**	***Viruses***

(*continued on next column*)

(*continued*)

➢ **Clade**	*Riboviria*
➢ **Kingdom**	*Orthornavirae*
➢ **Phylum**	*Pisuviricota*
➢ **Class**	*Pisoniviricetes*
➢ **Order**	*Nidovirales*
➢ **Suborder**	*Cornidovirineae*
➢ **Family**	*Coronaviridae*
➢ **Subfamily**	*Orthocoronavirinae*
➢ **Genus**	*Betacoronavirus*
➢ **Subgenus**	*Sarbecovirus*
➢ **Species**	*Severe acute respiratory syndrome-related coronavirus*
➢ **Strain**	*Severe acute respiratory syndrome coronavirus 2*

Due to an emergency outbreak, currently, only vaccines of several types have been made available with respect to various necessary guidelines to the people across the globe and it has shown the fine good response by producing antibodies against 2019-nCoV but along with it, there is an also a need for a proper drug targeting against this virus too thereby inhibiting its mechanism of survival rate. There is quite a large number of specifically approved drugs being available with us for treating various types of infections which blocks and inhibits the mechanism rate of their survival and this can be easily sorted out with

* Corresponding author. Amity Institute of Biotechnology, Amity University Rajasthan, Jaipur, 303002, Rajasthan, India.
E-mail addresses: shrutika.r.sakpal@gmail.com, shrutika.sakpal@iscm.ac.in (S. Sakpal).

https://doi.org/10.1016/j.jics.2022.100571
Received 30 November 2021; Accepted 6 June 2022
Available online 15 June 2022

Abbreviations

2019-nCoV	2019-novel Corona Virus
aa	Amino acids• FDA: Food and Drug Administration
ICTV	International Committee on Taxonomy of Viruses
MDS	Molecular Dynamic Simulation
MERS	Middle East respiratory syndrome
MSA	Multiple Sequence Alignment
SARS-1	*Severe acute respiratory syndrome coronavirus 1*
WHO	World Health Organisation

needed for activating the membrane fusion domain once infectious agent entry into the target cells. The S-protein binds to the ACE2 through the Receptor Binding Domain (RBD) region of the S1 monetary unit that mediates the infectious agent attachment to the host cells within the kind of a trimer. Underneath low pH, the S1 monetary unit of the 2019-nCoV binds with the ACE2 to market the formation of endosomes, that activates infectious agent fusion (fusion of the infectious agent membrane and therefore the host cell wall, leading to the discharge of the infectious agent ordering into the host cell) [5].

Since, spike protein of 2019-nCoV is a key factor for viral infection it hallmarks as a potential therapeutic target for the drug molecules through binding that can be achieved by molecular docking as it is an essential tool in structural biology and in designing drugs.

Table 1
Data of Surface Glycoprotein of Top 5 Affected countries with 2019-nCoV obtained through the World Health Organisation (WHO) source and Sr.No.6 denotes the data of China which is kept as a control system since the infection has been reported first from China [3].

Sr.No.	Accession No.	Country.	Release Date	Length	Protein	Isolation Source
1	QNN95017	USA, Florida	20-08-2020	1273	Surface glycoprotein	Human
2	QMT98140	Brazil	20-07-2020	1273	Surface glycoprotein	Human
3	QNN87974	India	03-09-2020	1273	Surface glycoprotein	Human
4	QNE73229	Russia	17-08-2020	1273	Surface glycoprotein	Human
5	QIS60288	Peru	31-03-2020	1273	Surface glycoprotein	Human
6	YP_009724390	China	12–2019	1273	Surface glycoprotein	Human lung

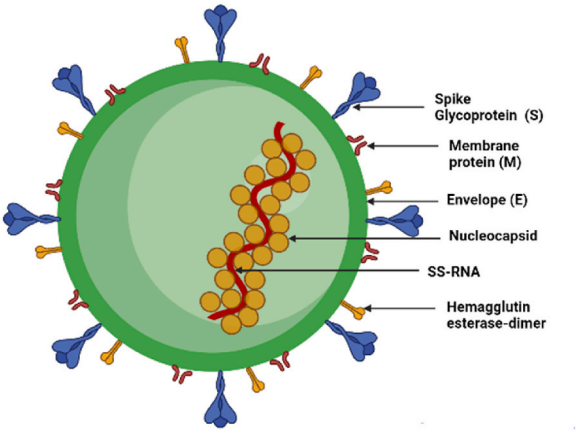

Fig. 1. Structure of 2019-nCoV created in BioRender [5].

the help of Molecular Docking and Simulation which helps in predicting the preferred orientation of the one molecule with a second molecule when bound to each other forming a stable Protein-Ligand complex in the output form of lowest Binding Affinity (Kcal/mol) that can be. achieved through various molecular modeling software and providing a result within a short period of time as compared to earlier traditional methods [2].

The size of the S-protein contains 180–200 kDa comprising of extracellular N-terminus, a transmembrane domain (TM) anchored within the infective agent membrane, and a short intracellular C-terminal segment. the whole length of S-protein contains 1273 amino acids (aa) comprising of single amide amino acids (1–13 aa) that area unit situated at the N-terminus, the S1 monetary unit (14–685 aa residues); the S2 monetary unit (686–1273 aa residues); the last 2 regions area unit answerable for binding the receptor and also the fusion membrane, respectively. The S-protein trimer visually forms a characteristic bulbous, crown-like halo encompassing the infectious agent particle. The S1 and S2 subunits type a bulbous head and stalk region (Fig. 1 and 2). In its native state, the 2019-nCoV virus exists in inactive precursor type. throughout the virus infection, the target cell proteases activate the S-protein by cleaving it into the S1 and S2 subunits that area unit

2. Materials and method (Fig. 3)

2.1. Multiple sequence alignment

Multiple Sequence Alignment (MSA) is generally the alignment of the three or more three biological sequences generally of protein, DNA, or RNA. Since 2019-nCoV has been declared pandemic so it was necessary to analyze the protein sequence alignment for the available structures and to determine the mutation variation rate. According to World Health Organisation (WHO) report the top five countries that were deadly affected by this pathogen were the USA, Brazil, India, Russia, and Peru (the position of the country may change according to the affected number of individuals which are updated daily). The FASTA sequence of these respective five countries was collected through NCBI and was aligned through Clustal Omega Tool along with China's FASTA sequence [7]. which was kept as a control as the 2019-nCoV emerged from China according to the previously available reports. The obtained result did not show a large variation in percent identity amongst the aligned sequences, so it was decided to go ahead and perform the molecular docking of the 2019-CoV Spike protein [8–10].

2.2. Target protein/macromolecule

The 2019-nCoV Spike protein (PDB ID- 6VXX Closed State) was obtained from Zhang Lab's I-Tasser site (https://zhanglab.ccmb.med.umich.edu/I-TASSER/) [11–13] in.pdb format (Figs. 4 and 5). PDB is a worldwide archive for the crystal structures of biological macromolecules. It comprises a resolution size of 2.80 Å obtained through electron microscopy; Spike Glycoprotein homopolymer Chains A, B, C, Oligo-saccharides (2-acetamido-2-deoxy-beta-D-glucopyranose-(1–4)-2-acetamido-2-deoxy-beta-D-glucopyranose) of which only Chain A was selected. The native ligand associated with it was NAG (2-acetamido-2-deoxy-beta-D-glucopyranose). The selection of Chain A was achieved by using multiple sequence alignment through the Clustal Omega (Clustal Omega < Multiple Sequence Alignment < EMBL-EBI) where it was analyzed that all the Chains (A, B, C) showed 100% identity amongst each other [8–10].

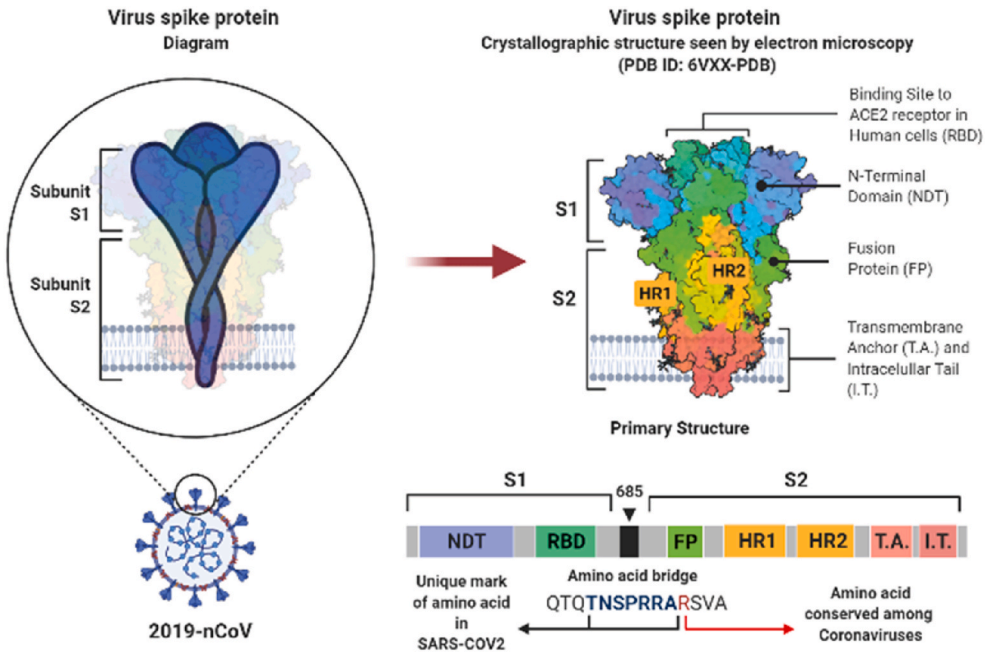

Fig. 2. Structure of the 2019-nCoV Spike [6].

2.3. Ligands

Observing it's deadly transmission globally, all the drug molecules viz. the ligands were selected by hypothesizing the previously available drug molecules that were approved for the treatment for MERS and SARS-1 infection and were obtained from the database of Drugbank (DrugBank Online. Detailed Drug and Drug Target Information) and ZINC database (ZINC docking.org) based on the obtained phylogenetic method through Mega X software for the respective SARS-1 and MERS where it was observed that these three viz. SARS-1, and SARS-2 belonged from the similar ancestors (" [17]"; "[18]."; [19–24].

2.4. Determination of active sites

The active sites were determined by the CASTp (**Computer Atlas of Surface Topography of Proteins)** web server (CASTp 3.0: Computed Atlas of Surface Topography of proteins (uic.edu)) [25] and Biovia Discovery Studio. Based on the obtained Active sites the dimension of the grid box for docking was selected in the following manner: (X: Y: Z) = (93 : 104: 134) in Angstrom [26].

2.5. Molecular docking

Ligand optimization was performed using Avogadro version 1.2; Autodock version 4.2 was used for protein optimization, by removing water and other atoms, and then by adding a polar hydrogen group. The molecular docking was performed through PyRx-0.8 software using Autodock-Vina. For performing the molecular docking all the selected ligands were converted into .pdbqt format by using Open Babel GUI. The specifically mentioned grid box dimension was selected for the loaded ligand and macromolecule and was allowed to dock. The obtained docked results having lower binding affinity and zero rmsd/ub; rmsd/lb was selected and was visualized and analyzed with the help of Biovia Discovery Studio (" [17]" [19,22,26,27];

2.6. Molecular dynamics simulation

The Molecular dynamic simulation for the top-scored ligand Paritaprevir (DB09297) was performed using Gromacs software [28–30] (version 2021.1) by using of GROMOS96 54a7 force field [27] from Automated Topology Builder (ATB) and Repository (version 3.0) server [31]. The triclinic box type (1.0 nm) was selected which occupied the volume of 46278 nm^3. The SPC (Simple point charge) water [32] was selected and the solvent molecules added were 1508333 with 7 Na^+ atoms to make the system neutral. Finally, the entire system comprised of 4537958 atoms [33].

The entire system was minimized by using the steepest descent integrator and at the 2948th step, the system was minimized. Thereafter the minimized system was equilibrated using two-phase: NVT (constant number of particles, volume, and temperature) ensemble in which the temperature of the system was allowed to reach at 300 K for a duration of 100 ps using the Leap-frog integrator followed by NPT (constant number of particles, pressure, and temperature) using a Leap-frog integrator with Parrinello-Rahman pressure coupler [33] for a duration of 100 ps. Finally, the entire well-equilibrated system was allowed to run for the production of molecular dynamics of 1000 frames data collection. The results were analyzed for the same protein and ligand complex in the form of a graph [34].

The molecular dynamic simulation was performed by using 64 bit Intel (R) Xeon (R) CPU @ 2.00 GHz with a total of 2 cores, 4 logical cores, and 1 compatible NVIDIA GPU (CUDA driver: 11.20) with a Tesla K80 processor.

3. Results

3.1. Percent Identity Matrix of the spike protein for SARS-1, MERS and 2019-nCoV

The data in the corresponding Fig. 6. states that the 2019-nCoV shares 30.70% similar sequence identity with MERS and 73.98% similar sequence identity with SARS-1 and thus it can be concluded that 2019-nCoV shares its ancestry more from the SARS-1 when compared with MERS which constitutes 30.70% similar sequence identity with respect to 2019-nCoV.

The data in the corresponding Fig. 7 describes the phylogenetic analysis and found that all variant sequences belong to the common ancestry with node length 0.00000 and it can be concluded that 2019-nCoV shares the most common ancestry with SARS-1 as compared

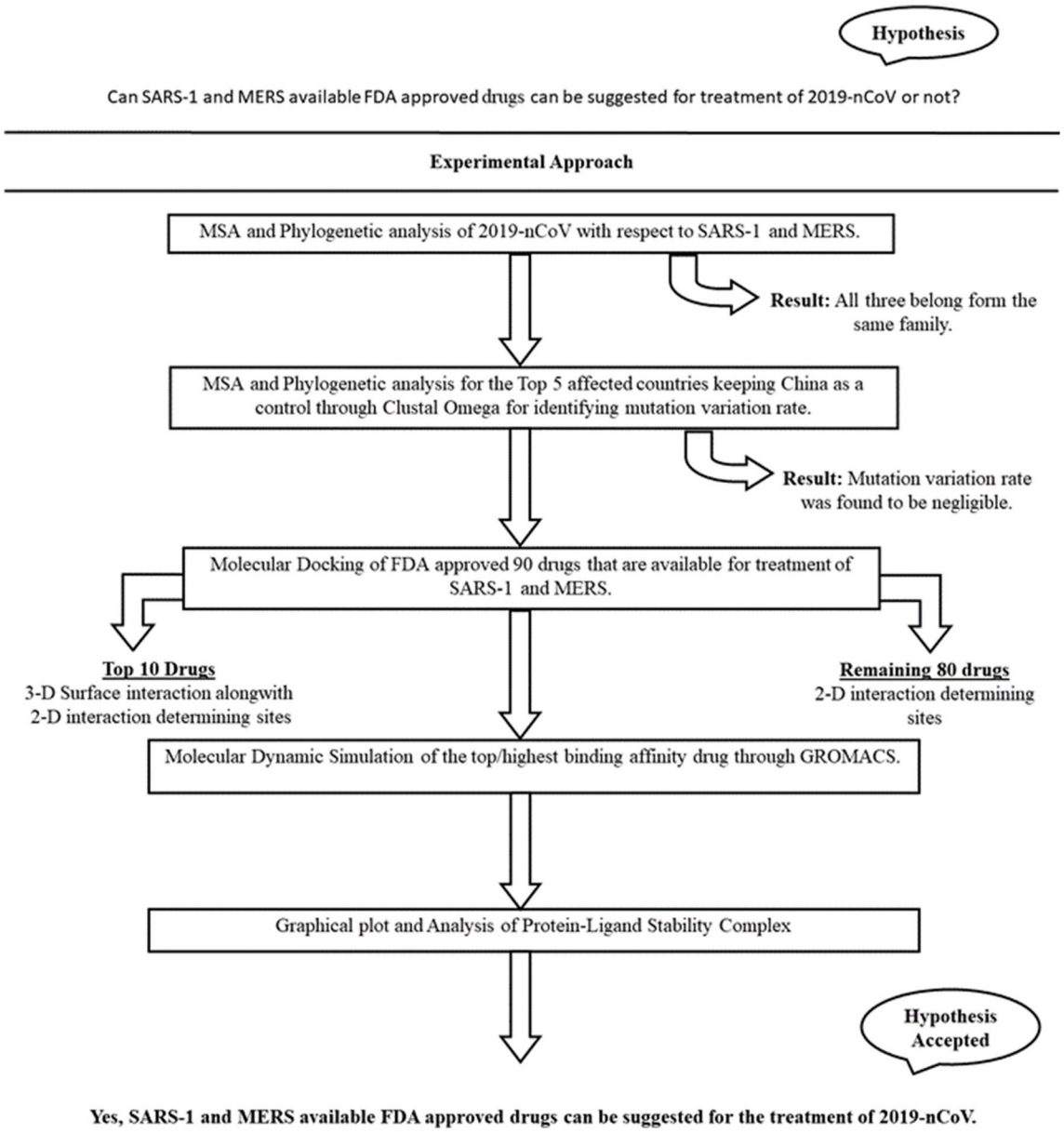

Fig. 3. Work-flow chart representing the overall methodology for MDS of Spike Protein (6VXX).

with MERS (see).

3.2. MSA output for the top 5 countries along with Yp_009724390 [China] keeping as a control system (Fig. 8)

3.3. Percent Identity Matrix for the top 5 countries obtained by performing MSA keeping YP_009724390[China] as a control system

The data in the corresponding Fig. 9. states that the top 5 countries do not show any mutation rate in their sequence but when compared with China, there is a slight variation or negligible variation in their sequence i.e., 99.92% Identity with respect to the top 5 countries.

The data in the corresponding Fig. 10. describe the phylogenetic analysis between top 5 countries keeping China (mentioned in blue colour) as a control system and found that all variant sequences belong to the common ancestry with node length 0.00000 but China has shown slight variation of 0.00039 node length due to the slight mutation occurred in Percent Identity Matrix mentioned in Fig. 9.

3.4. Three-dimensional surface image of top 10 ligands docked with 6VXX spike protein [18,20,21,23,24]

Fig. 11. represents the surface image of the docked ligand **Paritaprevir (DB09297)**. The Binding Affinity for this ligand has been found to be **-15.2 kcal/mol.** Paritaprevir is a direct-acting antiviral medication that is used for the treatment of chronic Hepatitis C virus infections (HCV), an infectious liver disease with a combination of other antiviral agents. The half-life of this drug has been found to be around 5.5 h. The molecular interactions of Paritaprevir with respect to Spike protein have been found in the following way:

- Conventional Hydrogen Bond – ASN:121;
- Unfavourable Positive-Positive – ARG:190;
- Pi-Sulfur – HIS:207;
- Pi-Pi Stacked – PHE:175;
- Alkyl, Pi-Alkyl – VAL:126, TYR:170, LEU:226, VAL:227

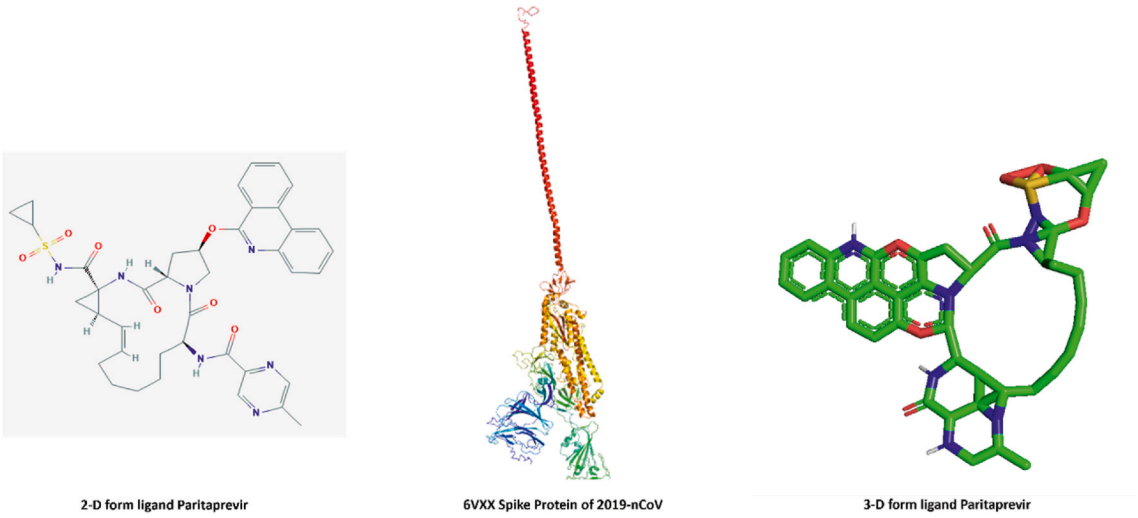

Fig. 4. 6VXX Spike protein and ligand paritaprevir.

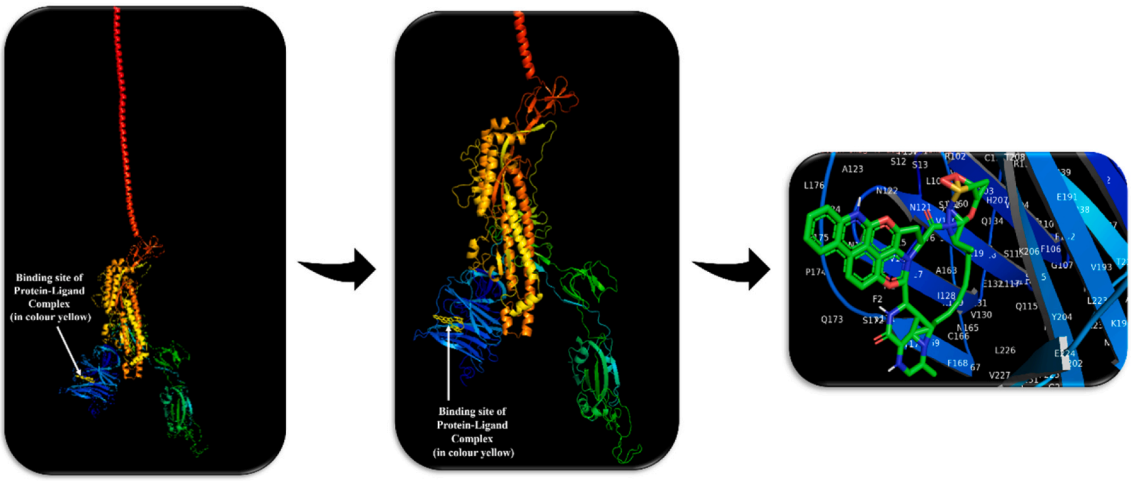

Fig. 5. Close view of Protein-Ligand Binding Site Complex obtained through PyMOL [14–16].

```
#
#
#  Percent Identity  Matrix - created by Clustal2.1
#
#

     1: ALM26400.1_MERS  100.00   30.76   30.70
     2: 5X5B_SARS-1       30.76  100.00   73.98
     3: 6VXX_2019-nCoV    30.70   73.98  100.00
```

Fig. 6. Percent Identity Matrix of the Spike Protein of MERS, SARS-1, and 2019-nCoV performed by MSA through Clustal Omega 2.1 version where **1:** ALM26400.1_MERS denotes MERS Spike Protein; **2:** 5X5B_SARS-1 denotes SARS-1 Spike protein; **3:** 6VXX_2019-nCoV denotes 2019-nCoV Spike Protein [8–10].

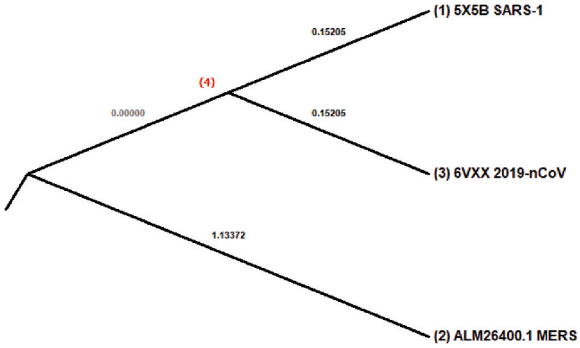

Fig. 7. The Phylogenetic Tree of the Spike Protein of SARS-1, 2019-nCoV and MERS (Source: WHO) obtained by the Clustal Omega MSA and thereby constructing the Phylogenetic tree through MSE (Minimal Evolution Method) with the help of MEGA X version 10.2.5 [35].

Fig. 12. represents the surface image of the docked ligand **Elbasvir (DB11574)**. The Binding Affinity for this ligand has been found to be **-12.1 kcal/mol.** Elbasvir is a direct-acting antiviral medication that is used for the treatment of chronic Hepatitis C virus infections (HCV), an infectious liver disease with a combination of other antiviral agents. The geometric mean apparent terminal half-life for elbasvir is 24 h in HCV-infected subjects. The molecular interactions of Elbasvir with respect to Spike protein have found in the following way:

- Carbon Hydrogen Bond – GLU:169, HIS:207;
- Pi-Sigma –LEU:226, VAL:227;
- Pi-Pi Stacked, Pi-Pi T-Shaped – PHE:168, TYR:170, PHE:192, HIS:207;
- Pi-Alkyl – VAL:126, LEU:226, VAL:227

Fig. 8. The obtained MSA output shows a variation at 614th position, indicated by a red box, where Aspartic Acid (D) has been replaced by Glycine (G) in the top 5 countries in which China is denoted by a period (.) to indicate the conservation of the D and G residues, which share weakly similar properties [8–10]. (For interpretation of the references to colour in this figure legend, the reader is referred to the Web version of this article.)

Fig. 13. represents the surface image of the docked ligand **Daclatasvir (DB09102)**. The Binding Affinity for this ligand has been found to be **-11.8 kcal/mol.** Daclatasvir is a direct-acting antiviral medication that is used for the treatment of chronic Hepatitis C virus infections (HCV), of genotype 1 and 3 infections with the combination of other antiviral agents. The half-life of this drug has been found to be around 12–15 h. The molecular interactions of Daclatasvir with respect to Spike protein have been found in the following way:

- Conventional Hydrogen Bond – TRP:104;
- Pi-Sigma – VAL:227;
- Pi-Pi Stacked, Pi-Pi T-Shaped – TYR:170, PHE:192, HIS:207;
- Pi-Alkyl – VAL:126, PHE:168, PHE:175, HIS:207, LEU:226, VAL:227

Fig. 14. represents the surface image of the docked ligand **Glycyrrhizic acid (DB13751)**. The Binding Affinity for this ligand has been found to be **-11.7 kcal/mol**. Glycyrrhizic acid is antiallergic, antivirals such as vaccinia virus, herpes simplex virus, Newcastle disease virus, and vesicular stomatitis virus. and anti-inflammatory activities. The half-life of this drug depending on the second elimination dose has been found to be around 3.5 h. The molecular interactions of Glycyrrhizic acid with respect to Spike protein has been found in the following way:

- Conventional Hydrogen Bond – ILE:101, TRP:104;
- Pi-Pi Stacked, Pi-Pi T-shaped – PHE:175, PHE:192, HIS:207;
- Alkyl – LEU:226, VAL:227

Fig. 15. represents the surface image of the docked ligand **Glecaprevir (DB13879)**. The Binding Affinity for this ligand has been found to be **-11.6 kcal/mol**. Glecaprevir is a direct-acting antiviral agent that targets the Hepatitis C virus (HCV) NS3/4A protease inhibitor. The half-life of this drug has been found to be around 6 h. The molecular interactions of Glecaprevir with respect to Spike protein have been found in the following way:

- Halogen bond with Fluorine – GLN:173, PRO:174;
- Pi-Pi Stacked – TYR:170;
- Pi-Alkyl – VAL:126, PHE:192, LEU:226, VAL:227

Fig. 16. represents the surface image of the docked ligand **Pibrentasvir (DB13878)**. The Binding Affinity for this ligand has been found to be **-11.5 kcal/mol.** Pibrentasvir is a direct-acting antiviral agent that targets the Hepatitis C virus (HCV) NS5A inhibitor. The half-life of this drug has been found to be around 13 h. The molecular interactions of Pibrentasvir with respect to Spike protein have found in the following way:

- Conventional Hydrogen Bond – CYS:538, SER:591, GLU:619;
- Carbon Hydrogen Bond – LYS:537, ASP:574, ILE:587;
- Halogen bond with Fluorine – PRO:589, CYS:590;
- Pi-Cation, Pi-Anion – LYS:557, ASP:586, GLU:619;
- Pi-Sigma – THR:553, VAL:551, THR:588;
- Pi-Pi Stacked – PHE:592;
- Pi-Alkyl – VAL:320, ALA:623, LYS:537, CYS:538, VAL:551

Fig. 17. represents the surface image of the docked ligand **Voxilaprevir (DB12026).** The Binding Affinity for this ligand has found to be **-11.3 kcal/mol**. Voxilaprevir is a direct acting antiviral agent used

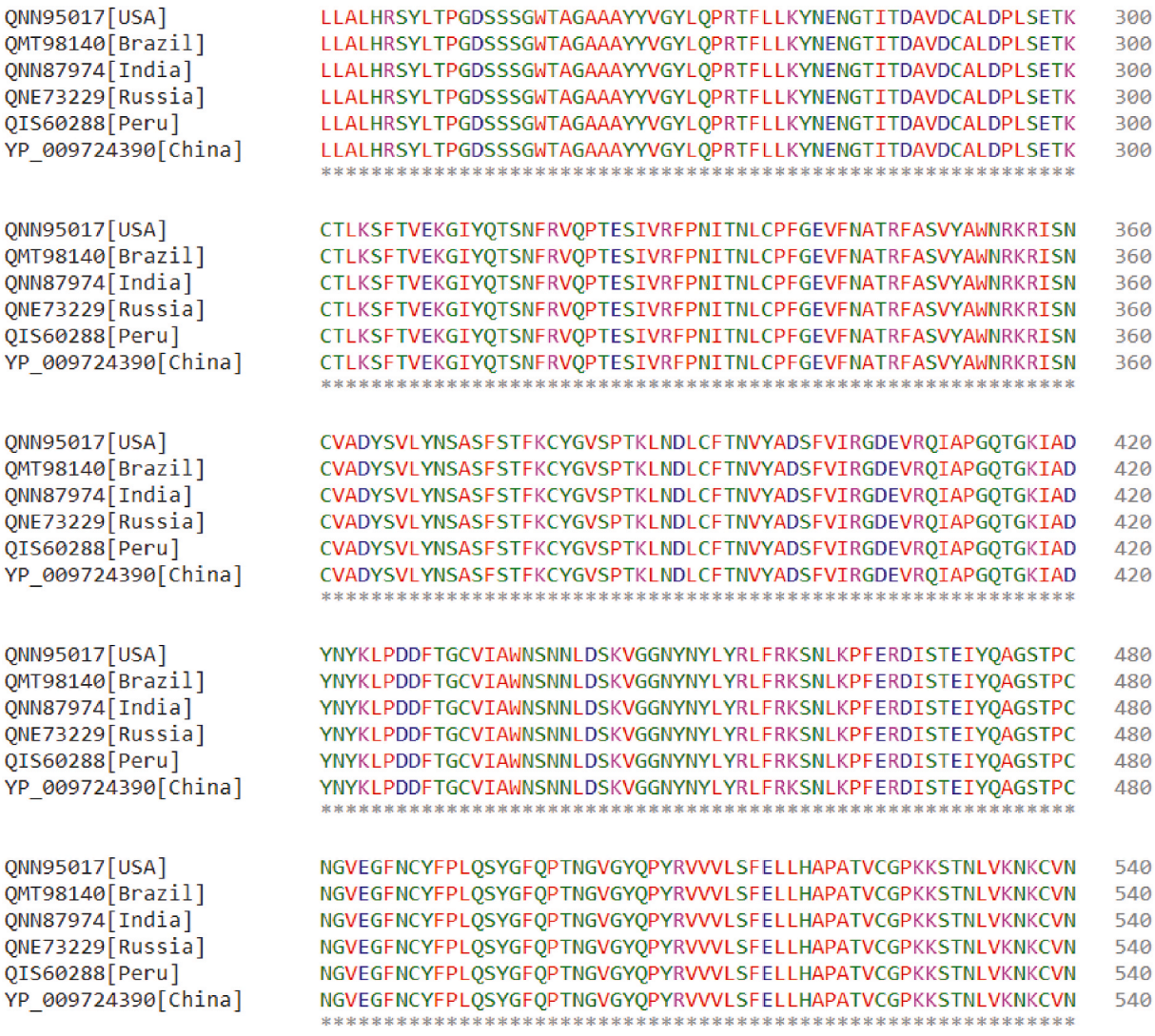

Fig. 8. (*continued*).

for curing the chronic Hepatitis C virus (HCV). The half-life of this drug has found to be around 33 h. The molecular interactions of Voxilaprevir with respect to Spike protein has found in the following way:

- Conventional Hydrogen Bond – ARG:190;
- Carbon Hydrogen Bond – PRO:174;
- Pi-Pi Stacked – TYR:170;
- Alkyl, Pi-alkyl – VAL:126, TYR:170, LEU:226, VAL:227

Fig. 18. represents the surface image of the docked ligand **Telaprevir (DB05521)**. The Binding Affinity for this ligand has found to be **-11.2 kcal/mol**. Telaprevir is a direct acting antiviral agent used for curing the chronic Hepatitis C virus (HCV) infections. The half-life of this drug has found to be of 4.0–4.7 h after a single dose of elimination and an effective half-life of 9–11 h at steady state. The molecular interactions of Telaprevir with respect to Spike protein has found in the following way:

- Conventional Hydrogen Bond – ASN:121, TYR:170;
- Pi-Sigma – SER:172;
- Pi-Pi Stacked, Pi-Pi T-shaped – PHE:175, HIS:207;
- Alkyl – ILE:119, MET:177, ILE:203, LEU:226

Fig. 19. represents the surface image of the docked ligand **Letermovir (DB12070)**. The Binding Affinity for this ligand has found to be **-11.2 kcal/mol**. Letermovir is an antiviral medication used to treat the CMV infections and disease in adult CMV-seropositive recipients of an allogeneic hematopoietic stem cell transplant (HSCT). The mean terminal half-life was observed to be 12 h following administration of Letemovir 480 mg IV once daily. The molecular interactions of Letermovir with respect to Spike protein has found in the following way:

- Pi-Sigma – VAL:126, LEU:226;
- Pi-Pi Stacked – PHE:175, PHE:192;
- Alkyl, Pi-Alkyl – ILE:119, VAL:126

Fig. 20. represents the surface image of the docked ligand **Grazoprevir (DB11575)**. The Binding Affinity for this ligand has found to be **-11 kcal/mol**. Grazoprevir is an antiviral medication used to treat the chronic Hepatitis C virus (HCV) infections. The geometric mean apparent terminal half-life for Grazoprevir has found to be 31 h in HCV-infected subjects. The molecular interactions of Grazoprevir with respect to Spike protein has found in the following way:

- Carbon Hydrogen Bond – GLU:96, TYR:170;
- Pi-Pi Stacked – PHE:192;
- Alkyl, Pi-Alkyl – VAL:126, TYR:170, LEU:226, VAL:227

The list of remaining (80) docked serially ligands with respect to

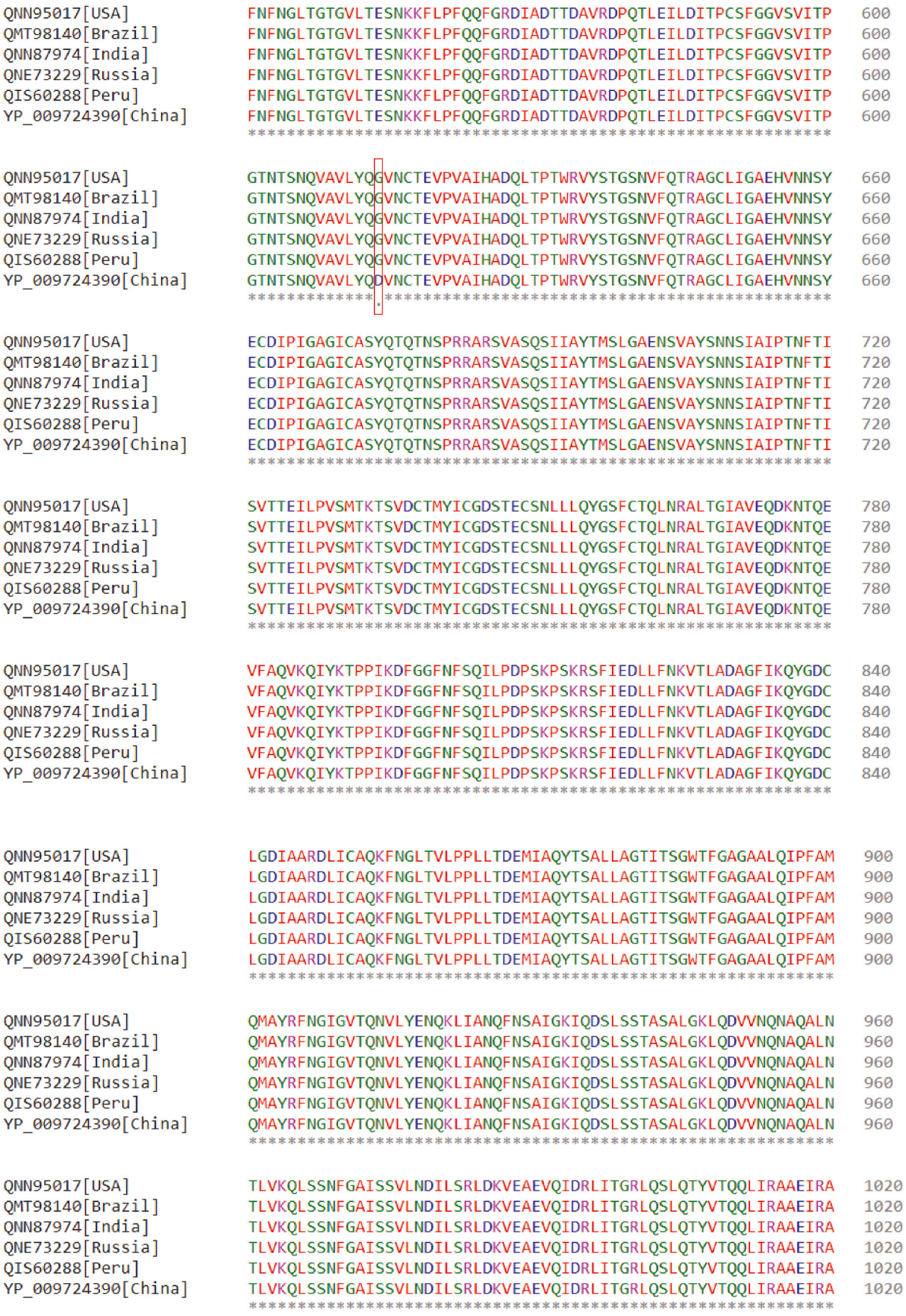

Fig. 8. (*continued*).

```
QNN95017[USA]          SANLAATKMSECVLGQSKRVDFCGKGYHLMSFPQSAPHGVVFLHVTYVPAQEKNFTTAPA   1080
QMT98140[Brazil]       SANLAATKMSECVLGQSKRVDFCGKGYHLMSFPQSAPHGVVFLHVTYVPAQEKNFTTAPA   1080
QNN87974[India]        SANLAATKMSECVLGQSKRVDFCGKGYHLMSFPQSAPHGVVFLHVTYVPAQEKNFTTAPA   1080
QNE73229[Russia]       SANLAATKMSECVLGQSKRVDFCGKGYHLMSFPQSAPHGVVFLHVTYVPAQEKNFTTAPA   1080
QIS60288[Peru]         SANLAATKMSECVLGQSKRVDFCGKGYHLMSFPQSAPHGVVFLHVTYVPAQEKNFTTAPA   1080
YP_009724390[China]    SANLAATKMSECVLGQSKRVDFCGKGYHLMSFPQSAPHGVVFLHVTYVPAQEKNFTTAPA   1080
                       ************************************************************

QNN95017[USA]          ICHDGKAHFPREGVFVSNGTHWFVTQRNFYEPQIITTDNTFVSGNCDVVIGIVNNTVYDP   1140
QMT98140[Brazil]       ICHDGKAHFPREGVFVSNGTHWFVTQRNFYEPQIITTDNTFVSGNCDVVIGIVNNTVYDP   1140
QNN87974[India]        ICHDGKAHFPREGVFVSNGTHWFVTQRNFYEPQIITTDNTFVSGNCDVVIGIVNNTVYDP   1140
QNE73229[Russia]       ICHDGKAHFPREGVFVSNGTHWFVTQRNFYEPQIITTDNTFVSGNCDVVIGIVNNTVYDP   1140
QIS60288[Peru]         ICHDGKAHFPREGVFVSNGTHWFVTQRNFYEPQIITTDNTFVSGNCDVVIGIVNNTVYDP   1140
YP_009724390[China]    ICHDGKAHFPREGVFVSNGTHWFVTQRNFYEPQIITTDNTFVSGNCDVVIGIVNNTVYDP   1140
                       ************************************************************

QNN95017[USA]          LQPELDSFKEELDKYFKNHTSPDVDLGDISGINASVVNIQKEIDRLNEVAKNLNESLIDL   1200
QMT98140[Brazil]       LQPELDSFKEELDKYFKNHTSPDVDLGDISGINASVVNIQKEIDRLNEVAKNLNESLIDL   1200
QNN87974[India]        LQPELDSFKEELDKYFKNHTSPDVDLGDISGINASVVNIQKEIDRLNEVAKNLNESLIDL   1200
QNE73229[Russia]       LQPELDSFKEELDKYFKNHTSPDVDLGDISGINASVVNIQKEIDRLNEVAKNLNESLIDL   1200
QIS60288[Peru]         LQPELDSFKEELDKYFKNHTSPDVDLGDISGINASVVNIQKEIDRLNEVAKNLNESLIDL   1200
YP_009724390[China]    LQPELDSFKEELDKYFKNHTSPDVDLGDISGINASVVNIQKEIDRLNEVAKNLNESLIDL   1200
                       ************************************************************

QNN95017[USA]          QELGKYEQYIKWPWYIWLGFIAGLIAIVMVTIMLCCMTSCCSCLKGCCSCGSCCKFDEDD   1260
QMT98140[Brazil]       QELGKYEQYIKWPWYIWLGFIAGLIAIVMVTIMLCCMTSCCSCLKGCCSCGSCCKFDEDD   1260
QNN87974[India]        QELGKYEQYIKWPWYIWLGFIAGLIAIVMVTIMLCCMTSCCSCLKGCCSCGSCCKFDEDD   1260
QNE73229[Russia]       QELGKYEQYIKWPWYIWLGFIAGLIAIVMVTIMLCCMTSCCSCLKGCCSCGSCCKFDEDD   1260
QIS60288[Peru]         QELGKYEQYIKWPWYIWLGFIAGLIAIVMVTIMLCCMTSCCSCLKGCCSCGSCCKFDEDD   1260
YP_009724390[China]    QELGKYEQYIKWPWYIWLGFIAGLIAIVMVTIMLCCMTSCCSCLKGCCSCGSCCKFDEDD   1260
                       ************************************************************

QNN95017[USA]          SEPVLKGVKLHYT  1273
QMT98140[Brazil]       SEPVLKGVKLHYT  1273
QNN87974[India]        SEPVLKGVKLHYT  1273
QNE73229[Russia]       SEPVLKGVKLHYT  1273
QIS60288[Peru]         SEPVLKGVKLHYT  1273
YP_009724390[China]    SEPVLKGVKLHYT  1273
                       *************
```

Fig. 8. (*continued*).

```
#
#
#  Percent Identity  Matrix - created by Clustal2.1
#
#

     1: QNN95017[USA]        100.00  100.00  100.00  100.00  100.00   99.92
     2: QMT98140[Brazil]     100.00  100.00  100.00  100.00  100.00   99.92
     3: QNN87974[India]      100.00  100.00  100.00  100.00  100.00   99.92
     4: QNE73229[Russia]     100.00  100.00  100.00  100.00  100.00   99.92
     5: QIS60288[Peru]       100.00  100.00  100.00  100.00  100.00   99.92
     6: YP_009724390[China]   99.92   99.92   99.92   99.92   99.92  100.00
```

Fig. 9. Percent Identity Matrix of the Top 5 affected countries (Source: WHO) with the 2019-nCoV obtained through the aligned FASTA sequence performed by MSA through Clustal Omega version 2.1 keeping- YP_009724390 [China] as a control system [8–10].

Spike protein with its respective ascending Binding Affinity (Kcal/mol) score has been described in Supplementary Table 1 in the tabular form with its two-dimensional (2-D) interactions.

3.5. Molecular dynamic simulation

From the above graph (Fig. 21.) it can be said that the system's energy was minimized at the 2948th step and the Potential energy was found to be −74170640 kJ/mol; whereas in the graph (Fig. 22.), it can be said that the temperature was quickly achieved to the target value at 300 K in 10 ps and it remained stable over the remainder of the equilibration (for 100 ps).

Over the equilibration time of 100 ps, the pressure value has fluctuated widely and an average pressure was found to be 5.37154 with an error estimation of 4.5 when it was set to 1 bar with 21.3276 bar root-mean-square deviation and −26.3204 bar total-drift whereas the running average of the density over the course of 100 ps found to be 970.584 kg/m^3 close to the experimental value of 1000 kg/m^3. From the density graph (Fig. 23.) it can be seen that the density values remain stable over time which indicates that the system is now well-equilibrated with respect to pressure and density.

Energy graph (Fig. 24.) was plotted with respect to number of frames and it was found that the average potential energy was found to be −6.24194e+07 kJ/mol whereas the average kinetic energy was found to be 1.13316e+07 kJ/mol and the average total energy was found to be −5.10879e+07 kJ/mol.

The hydrogen bond analysis was performed for protein and ligand separately of which it was found that Spike protein (6VXX) in water comprised of 1510164 donors and 1511883 acceptors whereas for the ligand (Paritaprevir) in water comprised of 1508336 donors and 1508347 acceptors (Fig. 25.).

The Root-mean-square deviation (RMSD) for the spike backbone protein (6VXX) ranges from 0.11996 to 0.84919 nm with an average of 0.538042 nm whereas the average RMSD for ligand (Paritaprevir) was

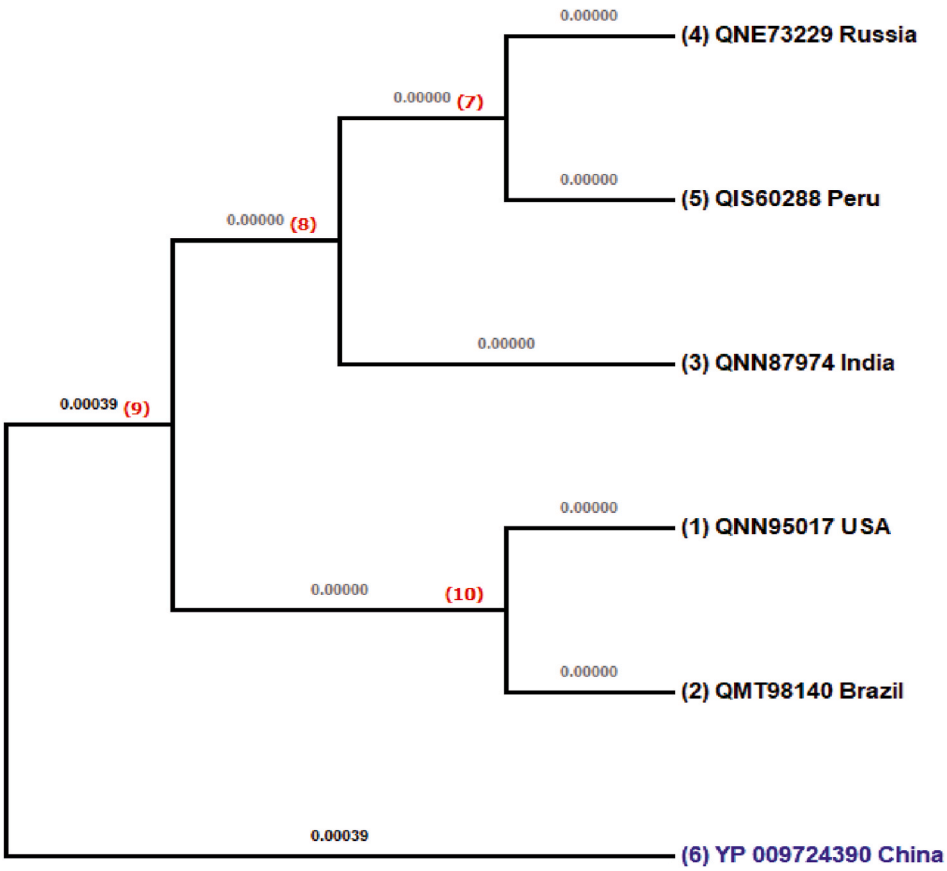

Fig. 10. Phylogenetic Tree of the Top 5 affected countries (Source: WHO) obtained by the Clustal Omega MSA and thereby constructing the Phylogenetic tree through MSE (Minimal Evolution Method) with the help of MEGA X version 10.2.5 [35].

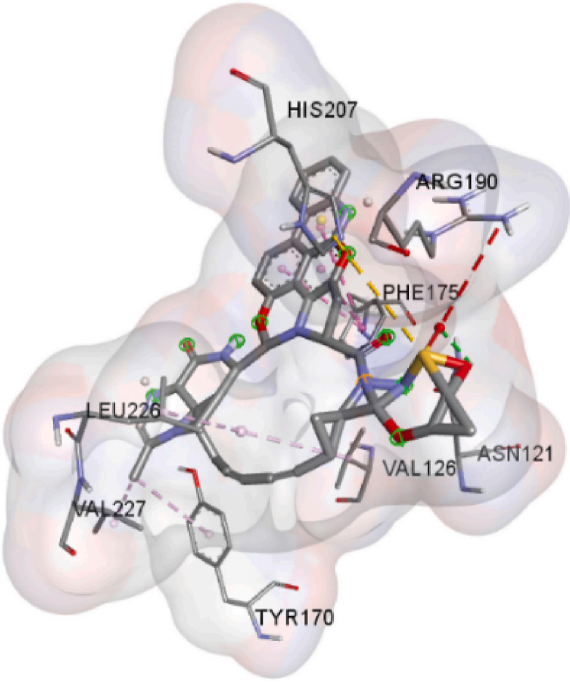

Fig. 11. Surface image of the docked ligand Paritaprevir (−15.2 kcal/mol).

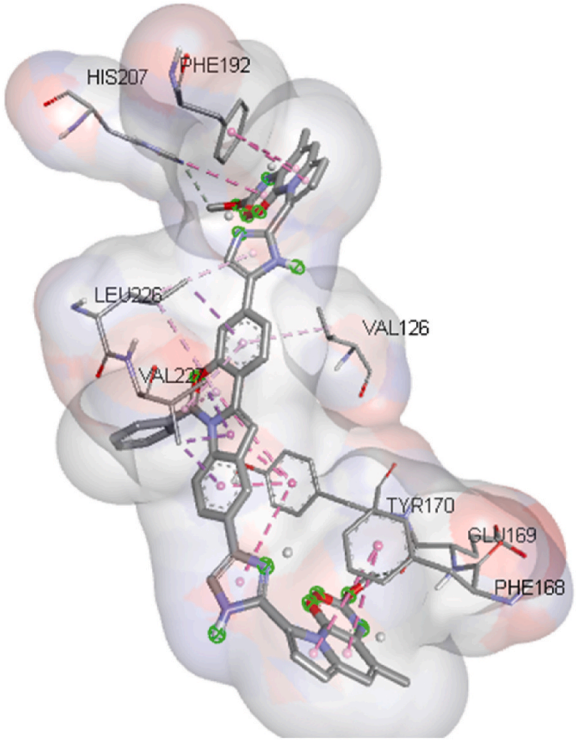

Fig. 12. Surface image of the docked ligand Elbasvir (−12.1 kcal/mol).

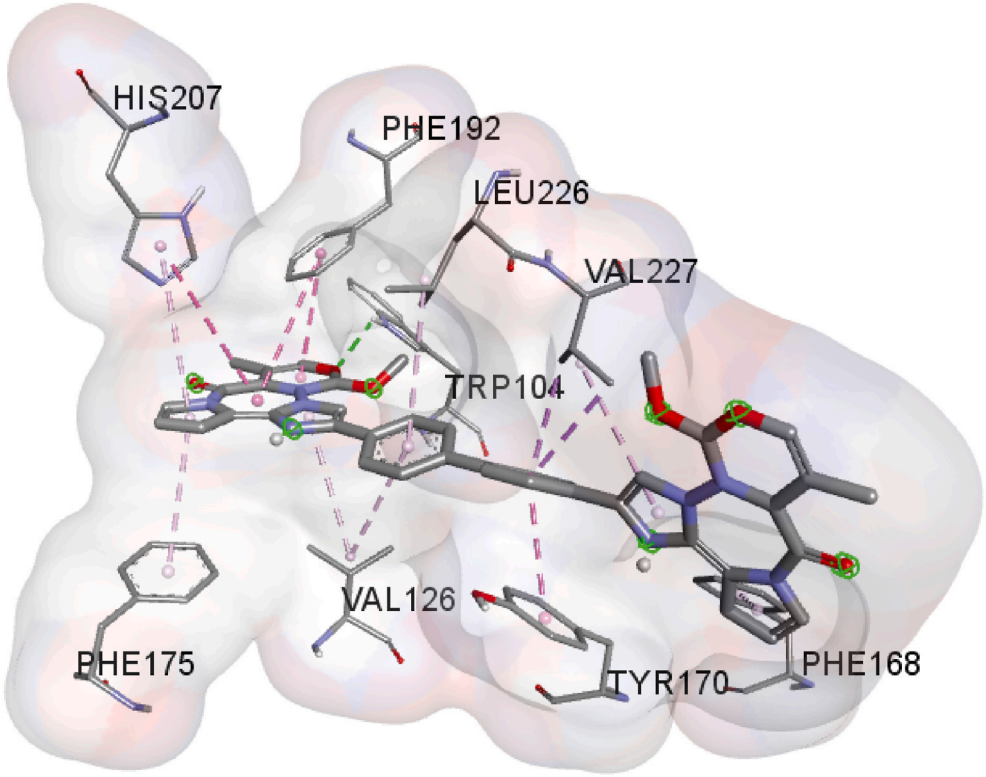

Fig. 13. Surface image of the docked ligand Daclatasvir (−11.8 kcal/mol).

found to be 0.241155 nm and the average RMSD for the Protein (6VXX) and ligand (Paritaprevir) complex was found to be 1.962278 nm for the resultant 1000 frames (Fig. 26.).

The Root-mean-square fluctuation (RMSF) helps to measure the flexibility of a residue and it is typically calculated for the C-alpha residues for the and it was found to be 0.325843 nm (Fig. 27.).

The Radius of Gyration helps to analyze the compactness of the system and for the entire system, it was found to be 18.76569 nm (Fig. 28).

We have also shown the graph of approved drugs and arranged them on the basis of their highest to lowest binding molecules among which Paritaprevir showed highest activity (Fig. 29).

4. Conclusion

Due to the Pandemic situation of 2019-nCoV currently, there is no approved potential drug that can be used as a therapeutic agent for treating this disease. However, some of the drugs have been taken into consideration which has shown to slow down the viral replication phase mechanism thereby which helps in decreasing the mortality rate of the patients. The currently available drug for treating the pandemic 2019-nCoV mainly acts on the main protease (M^{pro}) [36]. The main objective of this study was to examine the several approved drugs that have already been used for the treatment of SARS-1 and MERS since, 2019-nCoV shares the common ancestry relation amongst each other, and these drugs may be used to inhibit the Spike protein (S) of the 2019-nCoV since the S protein acts as a key factor by binding on ACE-2 receptors which helps in invading the viral entry into the host cell and thereby promoting the viral replication mechanism for increasing the viral load in host's body. The Binding Affinity of Paritaprevir (DB09297) bonds has shown the higher docking score i.e., −15.2 kcal/mol followed by Elbasvir, Daclatasvir, Glycyrhhizic acid, Pibrentasvir, Voxilaprevir, Telaprevir, Letermovir, Grazoprevir (Top 10 Ligands). The rest 80 ligands have also shown quite a good binding affinity score. Interestingly, it has also been found that these top 10 ligands are also being used for the treatment for curing the chronic Hepatitis C virus infection (HCV) along with the combination of other antiviral compounds. The revealed positive outcome of the hypothesis suggests that these top 10 drugs might serve as a potential target and the drug Paritaprevir can be suggested for the treatment for inhibiting the Spike Protein of 2019-nCoV. However, further research on different levels is necessary to investigate the potential use of these drugs.

Funding

This research did not receive any specific grant from funding agencies in the public, commercial, or not-for-profit sectors.

Web Resources.

1. WHO, https://covid19.who.int/
2. NCBI Virus, https://www.ncbi.nlm.nih.gov/labs/virus/vssi/#/sars-cov-2
3. ICTV Global Taxonomy, https://talk.ictvonline.org/
4. I-Tasser, https://zhanggroup.org/I-TASSER/
5. RCSB PDB, https://www.rcsb.org/
6. Clustal Omega, https://www.ebi.ac.uk/Tools/msa/clustalo/
7. CASTp, http://sts.bioe.uic.edu/castp/calculation.html

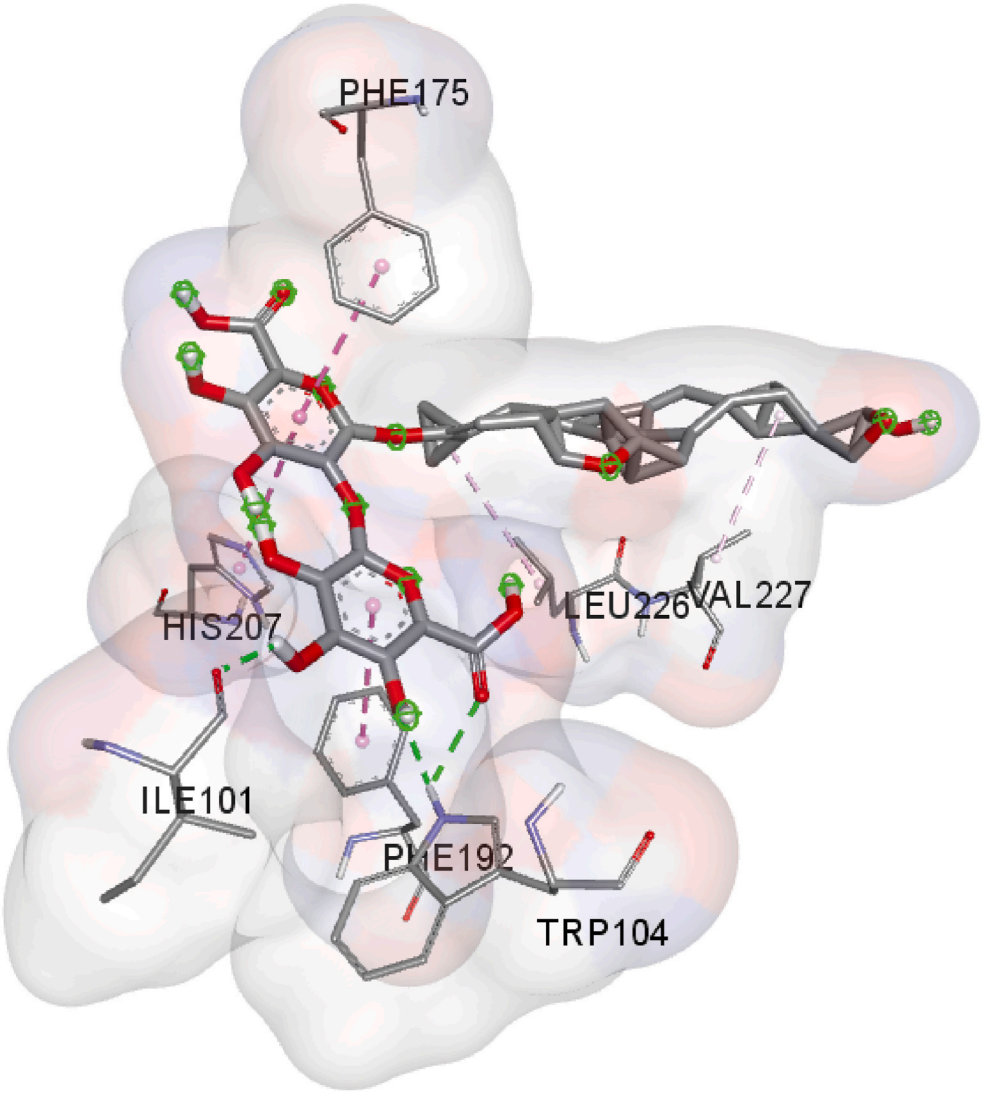

Fig. 14. Surface image of the docked ligand Glycyrrhizic acid (−11.7 kcal/mol).

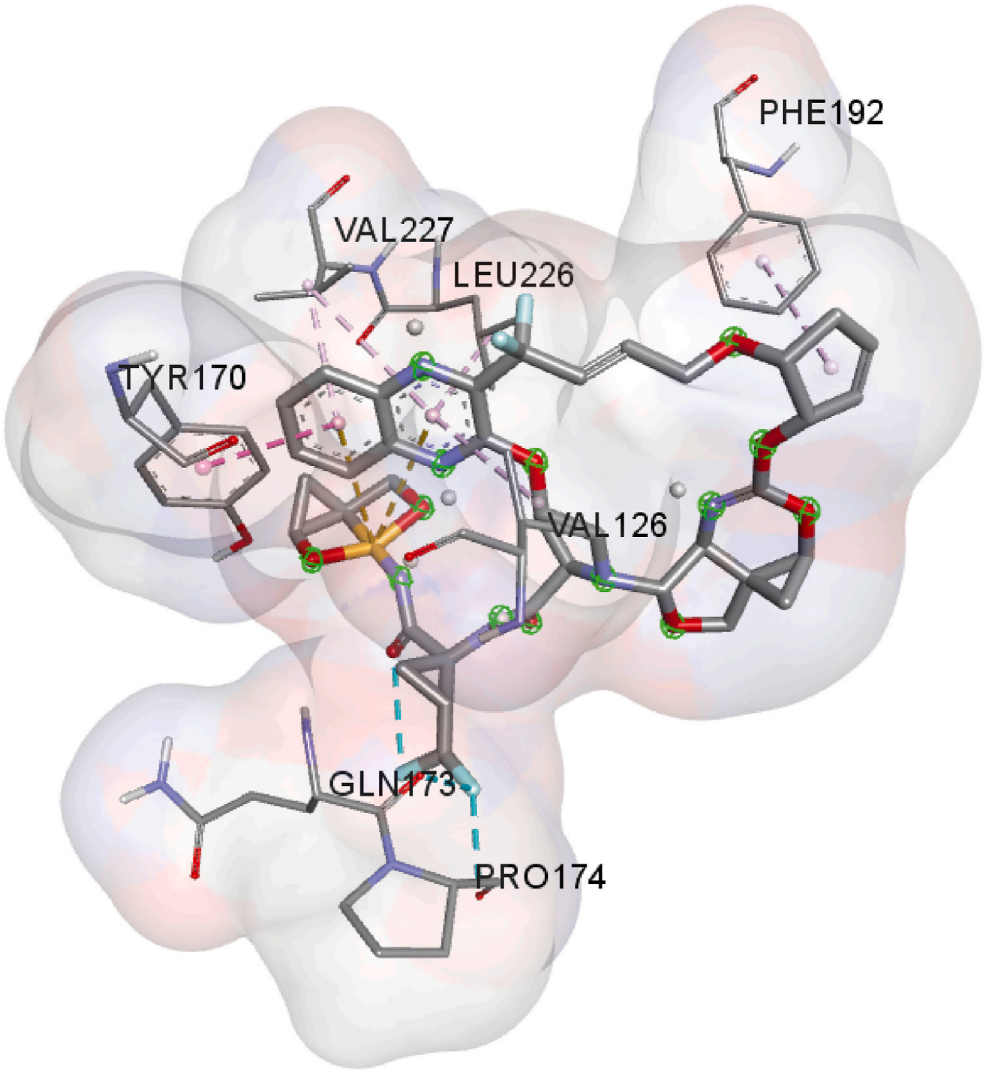

Fig. 15. Surface image of the docked ligand Glecaprevir (−11.6 kcal/mol).

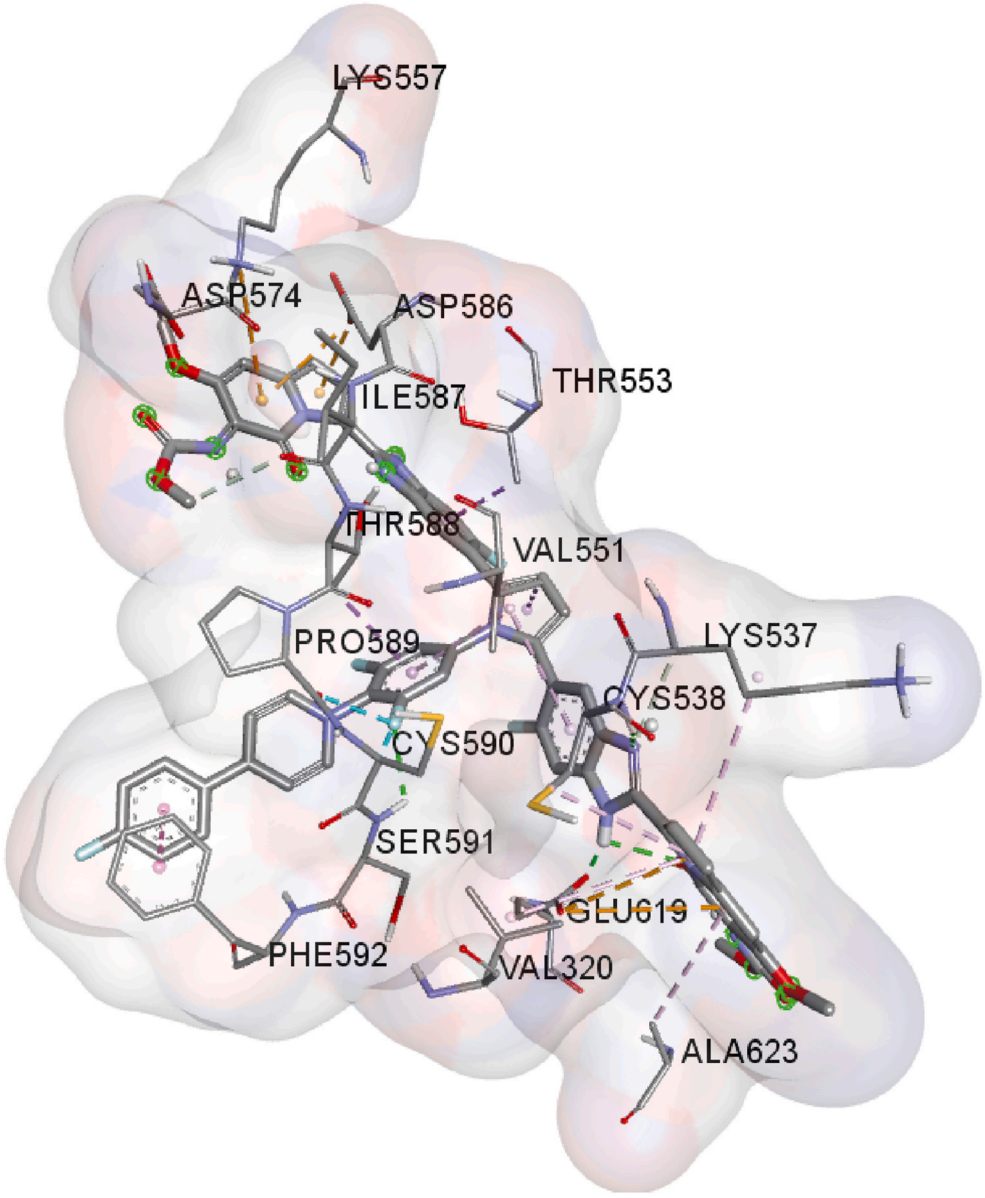

Fig. 16. Surface image of the docked ligand Pibrentasvir (−11.5 kcal/mol).

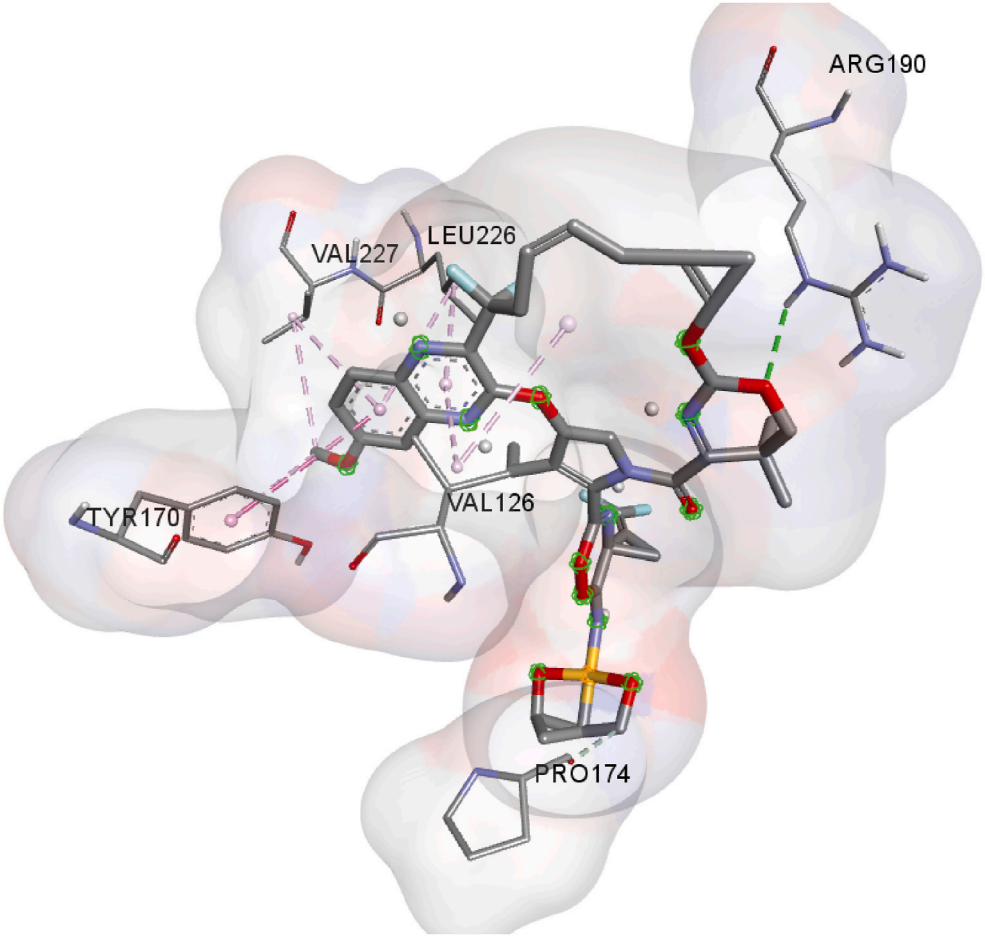

Fig. 17. Surface image of the docked ligand Voxilaprevir (−11.3 kcal/mol).

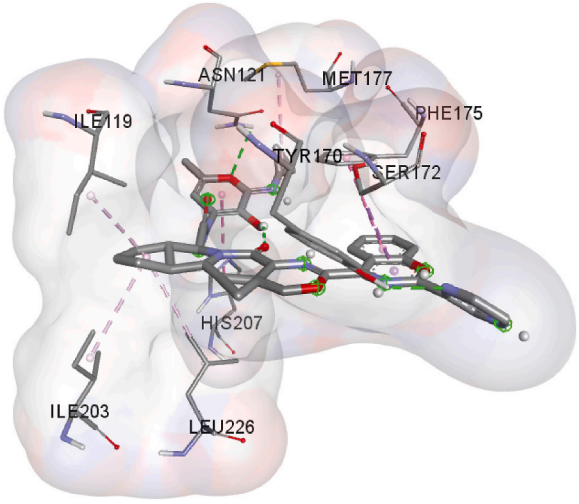

Fig. 18. Surface image of the docked ligand Telaprevir (−11.2 kcal/mol).

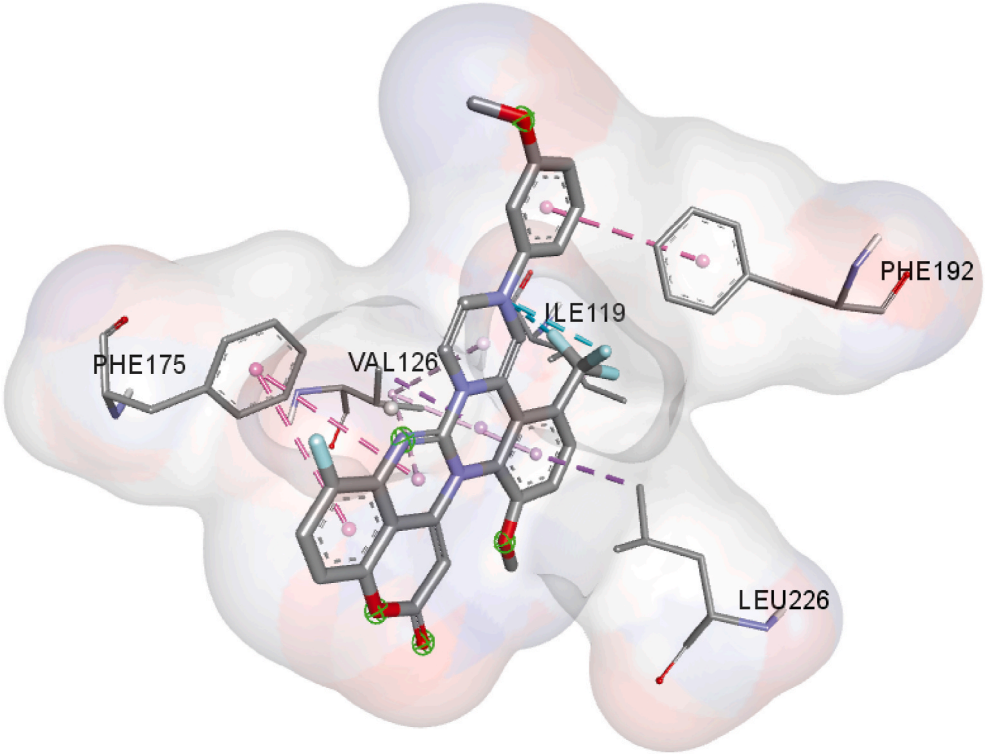

Fig. 19. Surface image of the docked ligand Letermovir (−11.2 kcal/mol).

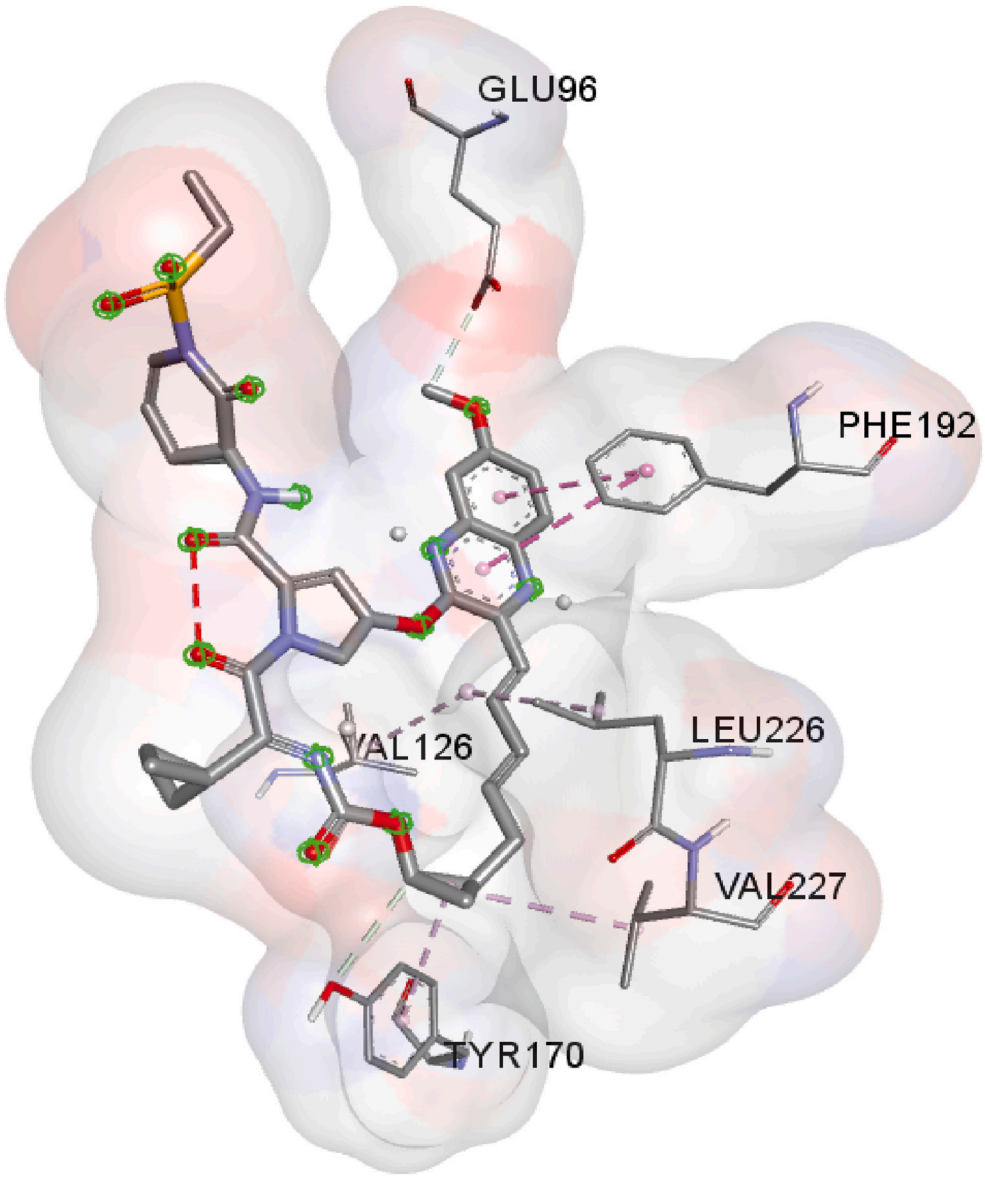

Fig. 20. Surface image of the docked ligand Grazoprevir (−11 kcal/mol).

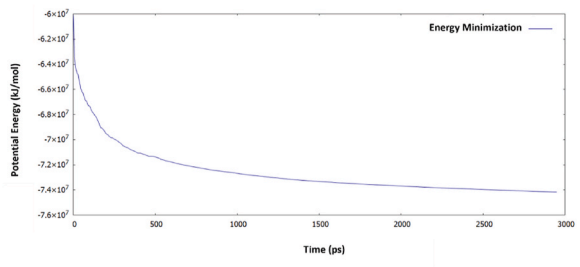

Fig. 21. Graph of Energy Minimization of the equilibrated system.

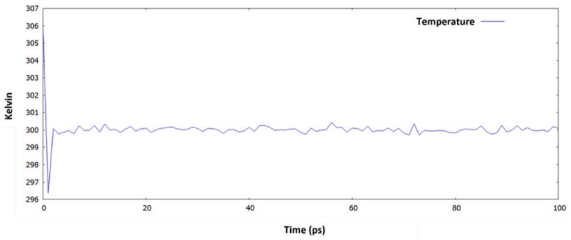

Fig. 22. Graph of Temperature of the equilibrated system.

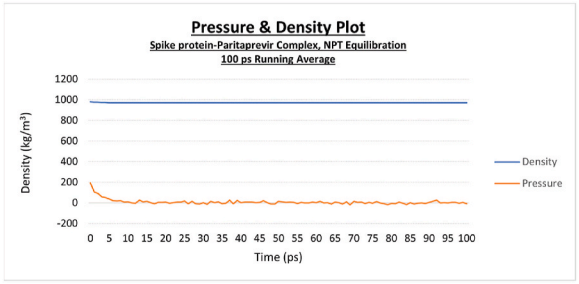

Fig. 23. Graph of Pressure and Density for the time 100 ps.

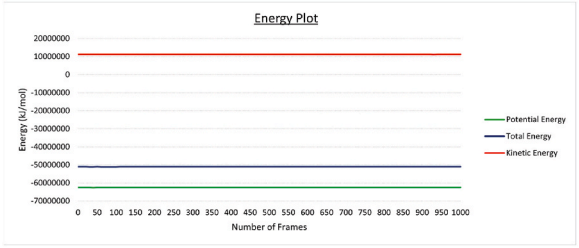

Fig. 24. Graph of Energy with respect to Number of Frames.

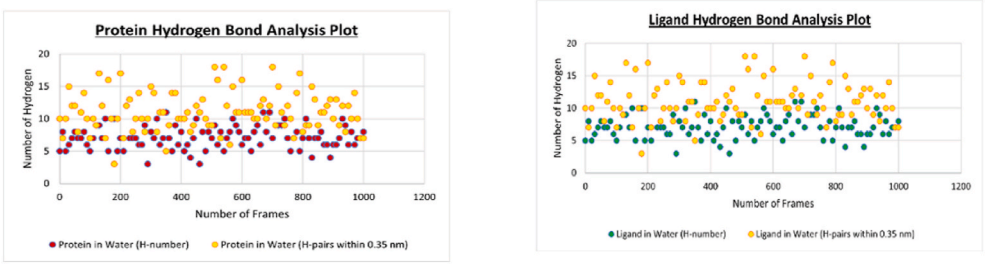

Fig. 25. Hydrogen Bond Analysis Plot with respect to Number of Frames.

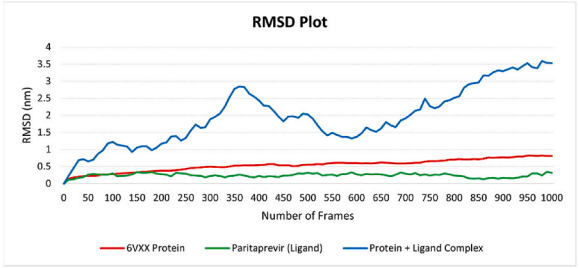

Fig. 26. Root-mean-square deviation (RMSD) plot with respect to Number of Frames.

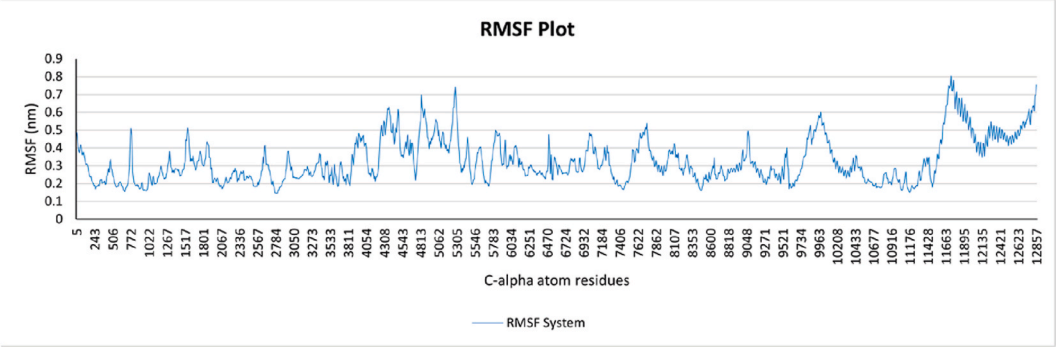

Fig. 27. Root-mean-square fluctuation (RMSF) plot with respect to Number of Frames.

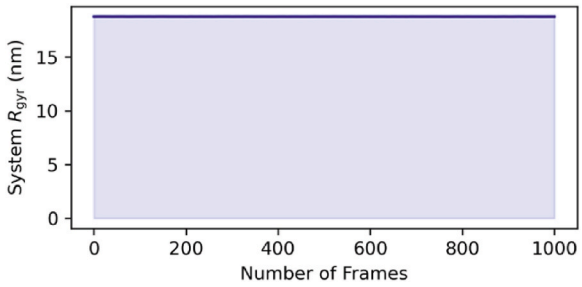

Fig. 28. Radius of Gyration plot with respect to Number of Frames.

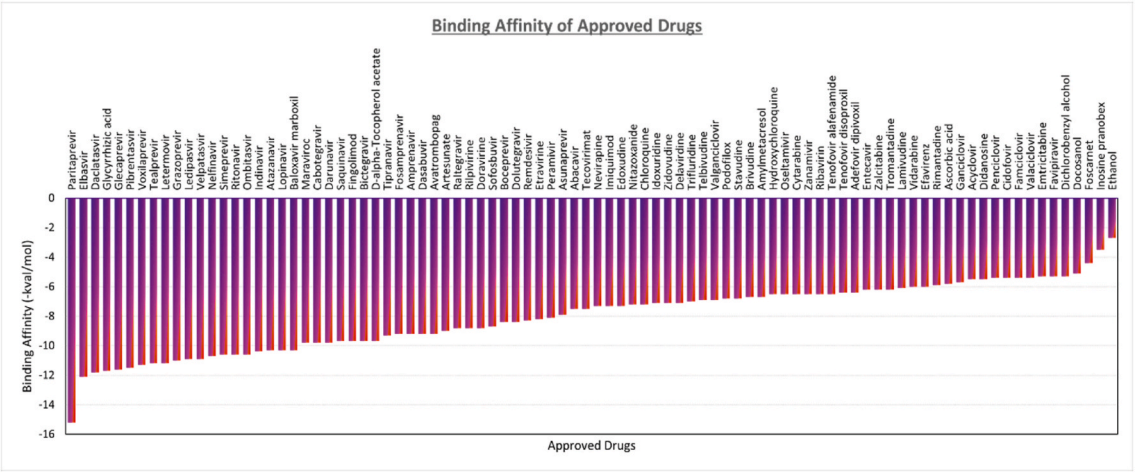

Fig. 29. Graph of Approved drugs with their respective Binding Affinity in chronological order where Paritaprevir shows the highest binding affinity of −15.2 kcal/mol and ethanol shows the lowest binding affinity of −2.7 kcal/mol.

Declaration of competing interest

The authors declare that they have no known competing financial interests or personal relationships that could have appeared to influence the work reported in this paper.

Acknowledgments

We would like to express our gratitude to Dr. Rupendra Jadhav (Coordinator) of the Department of Biotechnology, Dr. Homi Bhabha State University, The Institute of Science, Mumbai for providing our extraordinary support and encouraging us throughout the completion of the project. We would also like to thank our college "The Institute of Science Mumbai" a part of Dr. Homi Bhabha State University for granting us and allowing us to complete this project work. We would also like to acknowledge all the mentioned web resources for providing us the required datasets from their site.

Appendix A. Supplementary data

Supplementary data to this article can be found online at https://doi.org/10.1016/j.jics.2022.100571.

References

[1] A. Mittal, K. Manjunath, R.K. Ranjan, S. Kaushik, S. Kumar, V. Verma, COVID-19 Pandemic: Insights into Structure, Function, and hACE2 Receptor Recognition by SARS-CoV-2. PLoS Pathogens, 2020, https://doi.org/10.1371/journal.ppat.1008762.
[2] M. Shereen, S. Khan, A. Kazmi, N. Bashir, R. Siddique, Covid-19 Infection: Origin, Transmission, and Characteristics of Human Coronaviruses, 2020. Https://doi.org/10.1016/j.jare.2020.03.005 65.
[3] WHO COVID-19 Dashboard, World Health Organization, Geneva, 2020.
[4] International Committee on Taxonomy of Viruses (ICTV): https://ictv.Global/taxonomy/".
[5] Y. Huang, C. Yang, Xu X. feng, W. Xu, S. wen Liu, Structural and functional properties of SARS-CoV-2 spike protein: potential antivirus drug development for COVID-19, Acta Pharmacol. Sin. (2020), https://doi.org/10.1038/s41401-020-0485-4.
[6] Reprinted from "An In-depth Look into the Structure of the SARS-CoV2 Spike Glycoprotein", by BioRender, August 2020, retrieved from https://app.biorender.com/biorender-templates/figures/5e99f5395fd61e0028682c01/t-5f1754e62baea000aee86904-an-in-depth-look-into-the-structure-of-the-sars-cov2-spike-g Copyright 2021 by BioRender.
[7] Hatcher EL, Z.S.B.Y.B.O.N.E.O.Y.S.A.B.JR., n.d. Virus Variation Resource - Improved Response to Emergent Viral Outbreak.
[8] M. Goujon, H. McWilliam, W. Li, F. Valentin, S. Squizzato, J. Paern, R. Lopez, A new bioinformatics analysis tools framework at EMBL-EBI, Nucleic Acids Res. 38 (2010), https://doi.org/10.1093/nar/gkq313.
[9] H. McWilliam, W. Li, M. Uludag, S. Squizzato, Y.M. Park, N. Buso, A.P. Cowley, R. Lopez, Analysis tool web services from the EMBL-EBI, Nucleic Acids Res. 41 (2013), https://doi.org/10.1093/nar/gkt376.
[10] F. Sievers, A. Wilm, D. Dineen, T.J. Gibson, K. Karplus, W. Li, R. Lopez, H. McWilliam, M. Remmert, J. Söding, J.D. Thompson, D.G. Higgins, Fast, scalable generation of high-quality protein multiple sequence alignments using Clustal Omega, Mol. Syst. Biol. 7 (2011), https://doi.org/10.1038/msb.2011.75.
[11] J. Yang, Y. Zhang, I-TASSER server: new development for protein structure and function predictions, Nucleic Acids Res. 43 (2015), https://doi.org/10.1093/nar/gkv342.
[12] J. Yang, Y. Zhang, Protein structure and function prediction using I-TASSER, Curr. Protocol. Bioinformat. 52 (2015), https://doi.org/10.1002/0471250953.bi0508s52.
[13] Y. Zhang, I-TASSER server for protein 3D structure prediction, BMC Bioinf. 9 (2008), https://doi.org/10.1186/1471-2105-9-40.
[14] Schrödinger LLC, 2015a. The PyMOL Molecular Graphics System, Version~1.vol. 8..
[15] Schrödinger LLC, 2015c. The JyMOL Molecular Graphics Development Component, Versioñ1.vol. 8.
[16] Schrödinger LLC, 2015b. The AxPyMOL Molecular Graphics Plugin for Microsoft PowerPoint, Version~1.vol. 8..
[17] Avogadro: an open-source molecular builder and visualization tool. Version 1.20. http://avogadro.cc/.
[18] BIOVIA, Dassault Systèmes, Discovery Studio Visualizer, v21.1.0.20298, San Diego: Dassault Systèmes, 2020.
[19] M.D. Hanwell, D.E. Curtis, D.C. Lonie, T. Vandermeerschd, E. Zurek, G. R. Hutchison, Avogadro: an advanced semantic chemical editor, visualization, and analysis platform, J. Cheminf. 4 (2012), https://doi.org/10.1186/1758-2946-4-17.
[20] C. Knox, V. Law, T. Jewison, P. Liu, S. Ly, A. Frolkis, A. Pon, K. Banco, C. Mak, V. Neveu, Y. Djoumbou, R. Eisner, A.C. Guo, D.S. Wishart, DrugBank 3.0: a comprehensive resource for "Omics" research on drugs, Nucleic Acids Res. 39 (2011), https://doi.org/10.1093/nar/gkq1126.
[21] V. Law, C. Knox, Y. Djoumbou, T. Jewison, A.C. Guo, Y. Liu, A. MacIejewski, D. Arndt, M. Wilson, V. Neveu, A. Tang, G. Gabriel, C. Ly, S. Adamjee, Z.T. Dame, B. Han, Y. Zhou, D.S. Wishart, DrugBank 4.0: shedding new light on drug metabolism, Nucleic Acids Res. 42 (2014), https://doi.org/10.1093/nar/gkt1068.
[22] G.M. Morris, H. Ruth, W. Lindstrom, M.F. Sanner, R.K. Belew, D.S. Goodsell, A. J. Olson, Software news and updates AutoDock4 and AutoDockTools4: Automated docking with selective receptor flexibility, J. Comput. Chem. 30 (2009), https://doi.org/10.1002/jcc.21256.
[23] D.S. Wishart, Y.D. Feunang, A.C. Guo, E.J. Lo, A. Marcu, J.R. Grant, T. Sajed, D. Johnson, C. Li, Z. Sayeeda, N. Assempour, I. Iynkkaran, Y. Liu, A. MacIejewski, N. Gale, A. Wilson, L. Chin, R. Cummings, Di Le, A. Pon, C. Knox, M. Wilson, DrugBank 5.0: A major update to the DrugBank database for 2018, Nucleic Acids Res. vol. 46 (2018), https://doi.org/10.1093/nar/gkx1037.
[24] D.S. Wishart, C. Knox, A.C. Guo, D. Cheng, S. Shrivastava, D. Tzur, B. Gautam, M. Hassanali, DrugBank: a knowledgebase for drugs, drug actions and drug targets, Nucleic Acids Res. 36 (2008), https://doi.org/10.1093/nar/gkm958.
[25] W. Tian, C. Chen, X. Lei, J. Zhao, J. Liang, CASTp 3.0: computed atlas of surface topography of proteins, Nucleic Acids Res. 46 (2018), https://doi.org/10.1093/nar/gky473.
[26] O. Trott, A.J. Olson, AutoDock Vina: improving the speed and accuracy of docking with a new scoring function, efficient optimization, and multithreading, J. Comput. Chem. (2009), https://doi.org/10.1002/jcc.21334.
[27] N. Schmid, A.P. Eichenberger, A. Choutko, S. Riniker, M. Winger, A.E. Mark, W. F. van Gunsteren, Definition and testing of the GROMOS force-field versions 54A7 and 54B7, Eur. Biophys. J. 40 (2011), https://doi.org/10.1007/s00249-011-0700-9.
[28] M.J. Abraham, T. Murtola, R. Schulz, S. Páll, J.C. Smith, B. Hess, E. Lindahl, GROMACS: high performance molecular simulations through multi-level parallelism from laptops to supercomputers, SoftwareX 1–2 (2015), https://doi.org/10.1016/j.softx.2015.06.001.
[29] H.J.C. Berendsen, D. van der Spoel, R. van Drunen, GROMACS: a message-passing parallel molecular dynamics implementation, Comput. Phys. Commun. 91 (1995), https://doi.org/10.1016/0010-4655(95)00042-E.
[30] D. van der Spoel, E. Lindahl, B. Hess, G. Groenhof, A.E. Mark, H.J.C. Berendsen, GROMACS: fast, flexible, and free, J. Comput. Chem. 26 (2005), https://doi.org/10.1002/jcc.20291.
[31] A.K. Malde, L. Zuo, M. Breeze, M. Stroet, D. Poger, P.C. Nair, C. Oostenbrink, A. E. Mark, An automated force field Topology builder (ATB) and repository: version 1.0, J. Chem. Theor. Comput. 7 (2011), https://doi.org/10.1021/ct200196m.
[32] S. Miyamoto, P.A. Kollman, Molecular dynamics studies of calixspherand complexes with alkali metal cations: calculation of the absolute and relative free energies of binding of cations to a calixspherand, J. Am. Chem. Soc. 114 (1992), https://doi.org/10.1021/ja00036a015.
[33] J.S. Hub, B.L. de Groot, H. Grubmüller, G. Groenhof, Quantifying artifacts in ewald simulations of inhomogeneous systems with a net charge, J. Chem. Theor. Comput. 10 (2014), https://doi.org/10.1021/ct400626b.
[34] J. Racine, Gnuplot 4.0: a portable interactive plotting utility, J. Appl. Econom. 21 (2006), https://doi.org/10.1002/jae.885.
[35] S. Kumar, G. Stecher, M. Li, C. Knyaz, K. Tamura, Mega X: molecular evolutionary genetics analysis across computing platforms, Mol. Biol. Evol. 35 (2018), https://doi.org/10.1093/molbev/msy096.
[36] S.S. Suryawanshi, P.B. Jayannache, R.S. Patil, P. Ms, A. Sg, Molecular docking studies on screening and assessment of selected bioflavonoids as potential inhibitors of COVID-19 main protease, Asian J. Pharmaceut. Clin. Res. (2020), https://doi.org/10.22159/ajpcr.2020.v13i9.38485.